JOURNAL OF SOLID STATE CHEMISTRY **127,** 40–50 (1996)
ARTICLE NO. 0354

Evidences for the Formation of Chromium in the Unusual Oxidation State Cr(IV)

I. Chemical Reactivity, Microhomogeneity, and Crystal Structures of the Nonstoichiometric Channel Compounds $Tl_xCr_5Se_8$ ($0 \leq x \leq 1$)

W. Bensch, O. Helmer, and C. Näther

Institut für Anorganische Chemie, Universität Frankfurt, Marie-Curie-Strasse 11, 60439 Frankfurt a.M., Germany

Received November 28, 1995; in revised form August 2, 1996; accepted August 6, 1996

The topotactic redox reaction between $TlCr_5Se_8$ and bromine in acetonitrile leads to the formation of metastable samples with $0 \leq x < 1$ of $Tl_xCr_5Se_8$. Preparation at elevated temperatures yields for the first time a ternary transition metal chalcogenide crystallizing in the TlV_5S_8 type structure with a Tl content $x < 0.33$. As expected the topotactic redox reaction does not follow simple kinetics but is rather explained on the basis of the superposition of at least three different fundamental steps. EDAX investigations conducted on selected single crystals reveal that dependent on the deintercalation temperature, Tl is laterally inhomogeneous distributed along the needle axis which coincides with the crystallographic *b* axis. A pronounced maximum is observed at the middle of the crystals. In stoichiometric $TlCr_5Se_8$ the detailed analysis of the anisotropic displacement parameters of the Tl atoms reveal that the Tl atoms are displaced from the central position by about 0.26 Å. As a consequence the Tl atoms are coordinated by seven Se atoms in an irregular coordination polyhedron. Since the positions *x* 0 *z* are related by a center of symmetry they cannot be occupied simultaneously. Hence it must be assumed that $TlCr_5Se_8$ has a domain structure with local symmetry *Cm*. In the Tl poorer phases the refinement of the Tl atoms at the central position leads to unusual high U_{22} components. The observed microinhomogenity as well as an enhanced mobility and/or static disorder of the Tl atom within the channel may be responsible for this. The value for U_{11} decreases with decreasing Tl content whereas U_{33} is not affected. This observation is indicative for a different displacement of the Tl atoms from the central position. With respect to the possible reaction mechanisms, according to our structural investigations, the oxidation of monovalent Tl to trivalent Tl can be excluded. With decreasing Tl content the lattice parameters exhibit very anisotropic behavior, which is a direct consequence of the large changes of the interatomic Cr–Cr distances. The average ⟨Cr–Se⟩ as well as the nonbonding Se–Se distances are only slightly affected. These results suggest an oxidation of the formally trivalent Cr to the unusual tetravalent state Cr(IV), rather than the formation of valence band holes.

INTRODUCTION

Since the discovery of the ternary channel compound TlV_5S_8 (1) a large number of isostructural compounds with the formal composition $A_xM_5X_8$ have been prepared (A = Na, K, Rb, Cs, In, Tl; M = Ti, V, Cr; X = S, Se, Te) (1–15). For different ternary alkali metal chromium chalcogenides a structure classification from group–subgroup relations was proposed by Bronger *et al.* (3). In the overwhelming cases only preparation conditions and lattice parameters were reported. Only a few $A_xM_5X_8$ compounds were investigated with respect to their highly interesting physical properties (4, 6, 7, 13–20). TlV_5S_8 and TlV_5Se_8 are metals. Their crystal structures, their magnetic properties, and their electronic structures depend sensitively on the Tl content (12, 16). The isotypic Cr compounds $TlCr_5S_8$ and $TlCr_5Se_8$ are semiconductors or semimetals (17, 18). The magnetic properties of $TlCr_5S_8$ are typical for a low-dimensional system and are dominated by the formation of antiferromagnetically coupled Cr_2 dimers. As in the case of TlV_5S_8, the magnetic properties depend sensitively on the Tl content (18).

In the early 1980s Schöllhorn and co-workers demonstrated that in TlV_5S_8 the Tl atoms can electrochemically be de- and reintercalated leading to thermodynamic metastable samples (6). In a further study Ohtani and Onoue showed that Tl can also be removed via a topotactic redox reaction using iodine in donor solvents or a mixture of $AlCl_3/FeCl_3$ (7). Both authors reported that the lower limit for x was 0.33 in $Tl_xV_5S_8$. Within an ionic picture it was concluded that during the reaction Tl^+ is oxidized to Tl^{3+} and the charge of the host lattice remains constant (6, 7). Solid state NMR investigations gave hints for these conclusions (6, 21). Following the arguments of Schöllhorn *et al.* this topotactic redox reaction with electron/ion transfer can be formulated as

$$A^+[M_5X_8]^- \rightarrow A^{3+}_{1/3}[M_5X_8]^- + 2/3A^{3+} + 2/3\,e^-. \qquad [a]$$

0022-4596/96 $18.00

But interestingly enough a NMR study conducted by Ohtani and co-workers contradicts these findings (22, 23). It is also noteworthy that until now data about the reaction mechanism and about the kinetics of the deintercalation reactions of compounds with the TlV_5S_8 structure type are very rare.

Recently we investigated the $Tl_xV_5S_8$ system using X-ray photoemission experiments, magnetic susceptibility measurements, and single crystal X-ray investigations (16). We found no evidence for the formation of Tl^{3+}, but we observed significant changes in the core level region of V 2*p* and pronounced alterations of the magnetic properties indicative for a change of the charge of the host lattice (16). A systematic study of the mechanism of the redox reaction including ^{205}Tl NMR experiments of the $Tl_xV_6S_8$ system reveals that Tl is deintercalated as a Tl^+ species (24).

If the reaction follows [a], the most prominent changes should be observable in the environment of Tl since a Tl^{3+} is significantly smaller than Tl^+. But more seriously the reaction must stop at the composition $A_{0.33}M_5X_8$. Because this type of reaction is limited to *A* elements which can be oxidized during the redox reaction, it should be impossible to remove alkali ions from AM_5X_8. But interestingly enough Ohtani *et al*. demonstrated that Na can completely be removed from $NaCr_5Se_8$ using $AlCl_3$ (13). Therefore in addition to reaction [a] other reaction paths must be taken into account which may be formulated as

$$A^+[M_5X_8]^- \rightarrow A^+_{1-x}[M_5X_8]^{(1-x)-} + xA^+ + xe^- \qquad [b]$$

$$\rightarrow A^+_{1-x}[(M^{3+}_{5-x})(M^{4+}_x)(X^{2-}_8)]^{x-} \qquad [b1]$$

$$\rightarrow A^+_{1-x}[(M^{3+}_5)(X^{2-}_{8-x})(X^-_x)]^{x-}. \qquad [b2]$$

If the reaction proceeds by path [b], the oxidation takes place in the host lattice oxidizing either the metal [b1] or the chalcogen [b2]. In the former case metal ions in the unusual oxidation state M^{IV} are present. In the latter case the oxidation of chalcogen should result in the formation of valence band holes.

Because the question whether Tl or the host lattice is oxidized during the redox reaction is still open, we investigated $TlCr_5Se_8$ like a model system. Like many binary and ternary chromium chalcogenides, this compound exhibits interesting magnetic properties. It was reported that at about 50 K the localized magnetic moments order antiferromagnetically (4). The possible formation of Cr^{4+} and the interaction between Cr^{3+} and Cr^{4+} should result in interesting magnetic and electronic properties.

In part I of a series of contributions we report the results of the deintercalation experiments as well as investigations of the microhomogeneity of selected single crystals using SEM and EDAX. We also present the results of our X-ray investigations performed on different single crystals in the composition range $0.077 \leq x \leq 1$. Results of crystal structure Rietveld refinement performed on a powder of $Tl_{0.077}Cr_5Se_8$ are also presented.

Special attention is drawn to the question whether the X-ray experiments give evidence to decide whether the redox reaction follows the path [a], [b], [b1], or [b2].

In two future communications we will report the magnetic properties, low temperature crystal structural studies, and the electronic band structure of $Tl_xCr_5Se_8$ as a function of Tl content.

EXPERIMENTAL DETAILS

The ternary compound $TlCr_5Se_8$ was synthesized from the elements using the recipe given by Klepp *et al*. (2). The products consist of flat, up to 2-mm long black needles with a metallic luster. Single crystals with a reduced Tl content cannot be synthesized via a high temperature reaction. Hence the Tl poorer samples were prepared via a topotactical redox reaction using bromine in acetonitrile. For selected single crystals the reaction proceeded very slow and after 4 weeks we obtained crystals with a composition of $Tl_{0.78(2)}Cr_5Se_8$. After another 2 weeks the Tl content was reduced to $x = 0.61(2)$. Further reduction of Tl content yielded single crystals which were extremely brittle and not suitable for single crystal structure determination. Therefore, crystals with a lower Tl content were prepared in a slightly different way. The Br_2/CH_3CN solution was heated every second day to about 50°C over a period of 6 weeks. After each heating cycle the solution was cooled to room temperature and held at this temperature for 1 day. Crystals prepared in this way were mechanically stable. Until now all attempts to prepare single crystals with a Tl content significantly lower than about $x = 0.3$ were unsuccessful.

To monitor the chemical deintercalation as a function of time the reactions were also performed with ground and sieved samples (mesh <250). The Tl content of the solution was determined at defined time intervals using atomic absorption spectroscopy (AAS). After about 6 weeks samples with the composition $Tl_{0.04(2)}Cr_5Se_8$ were obtained. The deintercalation curve presented in Fig. 1 is the average of at least three runs.

The homogeneity of all samples was checked with X-ray powder diffractometry (STADIP, Cu$K\alpha$, λ = 1.54056 Å). X-ray powder data for the Rietveld refinement were recorded for a sample with nominal composition $Tl_{0.05}Cr_5Se_8$ between 5° and 118° 2Θ with a stepwidth of 0.01° and a counting time of 10 sec per step. Further details: Pearson VII function; 35 parameters; zero-point, overall-scale factor, 3 mixing and 3 profile-halfwide parameters; preferred orientation and peak asymmetry below 95° 2Θ were taken into account; refined lattice parameters, a = 18.4984(4) Å, b = 3.5633(1) Å, c = 8.8344(2) Å, β =

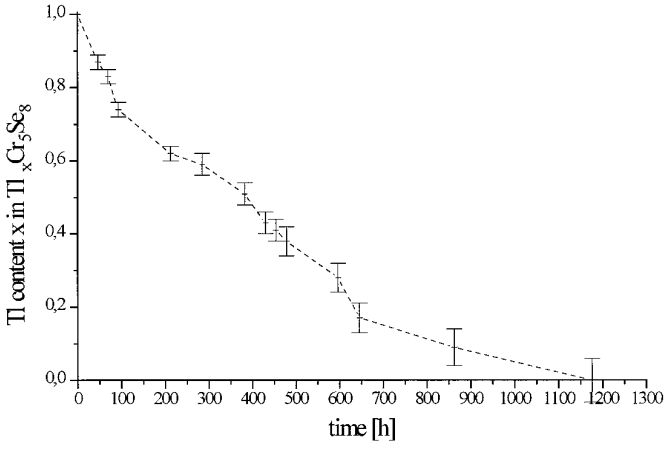

FIG. 1. Change of the Tl content in $Tl_xCr_5Se_8$ with time during the chemical redox reaction.

103.777(1)°, R_{wp} = 3.84%, R_{exp} = 1.35%, R_{Bragg} = 8.36%, S = 2.84. The difference Fourier synthesis of the structure without Tl showed the highest peak in 0, 0, 0. The Tl was placed on this site, the U_{iso} was fixed at 0.038, and the site occupation factor was let free to vary yielding a Tl content of x = 0.077(5) in $Tl_xCr_5Se_8$, in good agreement with the AAS result. Because individual interatomic bond distances derived from Rietveld refinements must be considered with some care, we only included the average $\langle M$–Se$\rangle$ distance and the Cr–Cr distances in Table 2. The refinement was carried out with the program package WYRIET.

Single crystal X-ray investigations were performed on a STOE AED II diffractometer using monochromized Mo$K\alpha$ radiation(λ = 0.7107 Å). Technical details of the data collections and selected results of the crystal structure refinements are summarized in Table 1. A numerical absorption correction was applied for all data sets. The weighting scheme was varied until no significant dependence upon sin θ/λ and F_o/F_{max} was observed.

The Tl content of the different single crystals was determined in the following way. The atoms of the host lattice were refined with anisotropic displacement parameters whereas the Tl atoms were refined with a freely varying isotropic displacement parameter. The site occupation factor (sof) of the Tl was also let free to vary. After determination of the sof for the Tl atoms, all atoms were refined anisotropically. The uncertainty of the Tl content is typically 0.02.

Selected crystals were studied with scanning electron microscopy (SEM) (JEOL 35 SM) and were also investigated with respect to their chemical composition using energy dispersive analysis of X-rays (EDAX) (ORTEC 2000 analysis system attached to the JEOL). For the EDAX studies (counting time at each step 100 sec), the crystals were divided into ten nearly identical parts. The composition at these points was calculated by assuming a constant Se content.

Lists of observed and calculated structure factors as well as extended tables of interatomic distances and angles are available on request.

RESULTS AND DISCUSSION

Chemical Reactivity

The change of Tl content as function of time is displayed in Fig. 1. Within about 300 h 50% of the Tl is deintercalated, but it takes another 900 h to reduce the Tl content to about 0. We analyzed the kinetics of the reaction with respect to normal kinetical laws, but as expected the reaction does not follow a simple order. This result can be explained on the basis of some simple considerations regarding the reaction mechanism. In the very first step bromine is reduced at the solid–solution interface. The most mobile species Tl is released from the solid and thallium monobromide is formed. Immediately after this initial reaction a donor acceptor complex of the form $TlBr \cdot Br_2 \cdots CH_3CN$ is built (24). This complex must be transported away from the surface of the solid. At this time a small concentration gradient appears in the solid and Tl atoms must diffuse to the surface to eqillibrate the chemical po-

TABLE 1
Technical Details of Data Aquisition and Some Refinement Results for Single Crystals of $Tl_xCr_5Se_8$ (x = 1, 0.78, 0.61, and 0.32)

x	1	0.78	0.61	0.32
a[Å]	18.712(4)	18.651(4)	18.619(5)	18.576(2)
b[Å]	3.614(1)	3.594(1)	3.583(1)	3.574(1)
c[Å]	8.969(3)	8.953(3)	8.943(2)	8.898(1)
β(°]	104.67(3)	104.41(3)	104.24(2)	103.99(1)
V[Å^3]	586.8(3)	581.3(3)	578.3(3)	573.1(3)
d_{calc} [g/cm^3]	6.204	6.006	5.835	5.543
$2\Theta_{max}$	60	55	55	60
N_o	634	438	533	680
N_p	48/46	45	46	46
x^a	0.00127(8)	—	0.00019(5)	0.00041(6)
y^b	0.0003	0.001	0.0003	0.0008
δF[e/Å^3]max.	2.3/4.4	2.6	1.9	2.6
min.	−2.0/−3.8	−3.7	−2.7	−1.8
R_F[%]	3.38/4.48	6.55	4.37	3.02
R_w[%]	3.31/4.31	5.67	3.99	3.15
GOOF	1.49/2.22	1.16	1.57	1.12
Tl U_{11}[Å$^2 \cdot 10^3$]	52(1)/130(1)	72(3)	54(1)	47(1)
Tl U_{22}[Å$^2 \cdot 10^3$]	33(1)/32(1)	117(6)	116(3)	60(1)
Tl U_{33}[Å$^2 \cdot 10^3$]	39(1)/39(1)	33(2)	37(1)	27(1)

Note. For x = 1 the first data of the refinement results are obtained with Tl in $x, 0, z$ and the results of the refinement with Tl in 0, 0, 0 (see text).
[a] Extinction correction: $F^* = F[1 + 0.002 \times F^2/\sin(2\Theta)]^{-1/4}$.
[b] Weighting scheme: $w^{-1} = \sigma^2(F) + yF^2$.

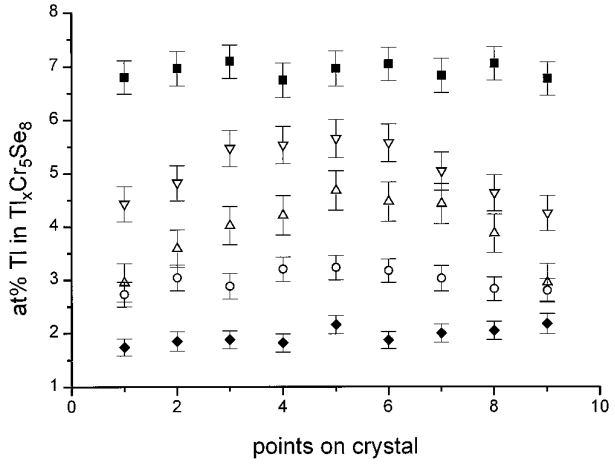

FIG. 2. Variation of the Tl content along the crystallographic *b* axis using EDAX point to point analysis performed on selected single crystals. Composition $Tl_xCr_5Se_8$ of the crystals from top to bottom: $x = 1$, $x = 0.78$, $x = 0.61$, $x = 0.4$, and $x = 0.26$.

tential. This diffusion proceeds in only one dimension, i.e., parallel to the crystallographic *b* axis. It is obvious that the fastest step of the reaction is the redox reaction itself and that the slowest part is the diffusion of Tl through the solid. It can be assumed that during the early steps of the redox reaction the number of defects is low enough so that the diffusion of Tl is not too strongly hindered, but with increasing time the subsequent delivery of Tl becomes more and more important.

Because the rate determining step is the diffusion of Tl, the velocity of the reaction sensitively depends on temperature and concentration of defects within the solid. It must also be kept in mind that the redox potential of the solid is changed during the reaction whereas the large excess of Br_2 in the solution leads only to a negligible change of the oxidizing power.

Microhomogeneity

As mentioned above, $TlCr_5Se_8$ crystallizes as long thin black needles. The needle axis coincides with the crystallographic *b* axis. We determined the Tl content of selected single crystals along the lateral direction using EDAX. The results of these investigations are displayed in Fig. 2. For the stoichiometric compound a homogeneous distribution of Tl is observed. Tl poorer crystals which were obtained via the chemical reaction at room temperature show a significant variation of the Tl content along the needle axis. The Tl content is highest in the middle and significantly lower at the ends of the crystals. A rough estimation of the variation of the composition along the needle axis of $Tl_{0.61}Cr_5Se_8$ yields $Tl_{0.45}Cr_5Se_8$ at the end and $Tl_{0.67}Cr_5Se_8$ in the middle of the crystal. Such large variations must lead to strong macroscopic strain and explains the brittleness of these crystals. In addition, this lateral microinhomogeneity should lead to enhanced anisotropic displacement parameters U_{22}. The inhomogeneous distribution of Tl along the needle axis may be caused by lattice defects which hinder the outdiffusion of the Tl atoms (25). In addition at room temperature the mobility of the Tl atoms is too low to achieve equilibrium. These assumptions are supported by the observations that crystals deintercalated at elevated temperatures or for very small crystals such a concentration gradient is absent. This is exemplified also in Fig. 2. The distribution of Tl along the needle axis shows no significant variation for $Tl_{0.4}Cr_5Se_8$ and $Tl_{0.26}Cr_5Se_8$ which were obtained via a topotactic redox reaction at elevated temperatures.

Attempts to achieve equilibrium by heating selected crystals with the compositions $Tl_{0.78(2)}Cr_5Se_8$ and $Tl_{0.61(2)}Cr_5Se_8$ at 475 K for several days were not successful. In all cases the crystals were destroyed and split into very small pieces. It is assumed that the high mechanical strain destroys the samples.

The Crystal Structure

The crystal structure of $TlCr_5Se_8$ is displayed in Figs. 3a and 3b. The coordination polyhedron about the Tl atom in both possible positions (see below) is shown in Figs. 4a and 4b. Selected interatomic distances are summarized in Table 2.

The crystal structure is built up of a 3-dimensional framework $^3_\infty[Cr_5Se_8]$ of $[CrSe_6]$ octahedra sharing edges and faces to form channels running parallel to the crystallographic *b* axis. The Tl atoms are confined within these channels. According to the results of Klepp *et al.* (2) the coordination polyhedron about Tl may be described as a bicapped distorted cube built up of 10 Se atoms.

The connection of the $CrSe_6$ octahedra via common edges and faces results in a displacement of the Cr atoms from the centers of the octahedra and alternating short and long Cr–Cr distances are found. The resulting quasi-tow-dimensional metal atom network is displayed in Fig. 5. A single zigzag chain made up from Cr2 atoms runs parallel to the crystallographic *b* axis and double zigzag chains of Cr1 and Cr3 atoms are parallel to the [001] plane.

A relatively short Cr–Cr distance of 3.057 Å is observed between the Cr atoms in the octahedra sharing faces. The Cr–Cr distances between Cr atoms within octahedra sharing common edges are significantly longer (Table 2). The lattice parameters of $TlCr_5Se_8$ and the interatomic distances are in good agreement with the values reported by Klepp *et al.* (2).

The crystal structure refinement of $TlCr_5Se_8$ with the Tl atoms in 0, 0, 0 results in an anisotropic displacement component U_{11} for the Tl atom ($B_{11} = 10.3$ Å^2) which is

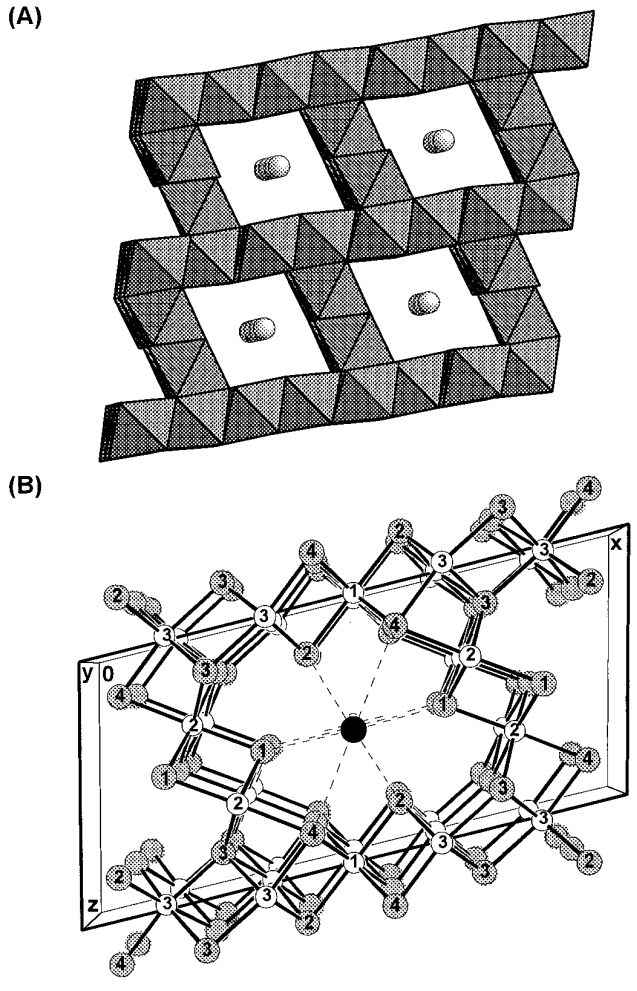

FIG. 3. Polyhedral representation of the crystal structure of $TlCr_5Se_8$ (A) and view of the unit cell showing the labeling of the atoms (B) (open circles, Cr atoms; shaded circles, Se atoms; black circle, Tl atom).

4 times larger than the values for U_{22} and U_{33}. A similar result was reported by (2). This observation indicates that the Tl atoms are displaced from the centers of the tenfold coordination polyhedron toward an edge of the polyhedron (see Fig. 4b). Refinement of the Tl atom with free varying x and z coordinates results in a significant reduction of the high U_{11} component (B_{11} = 4.11 Å^2) and a remarkable decrease in the reliability factors (see Table 1). The Tl atoms are shifted from the central position by about 0.26 Å and are now coordinated by 7 Se atoms in an asymmetric arrangement (see Fig. 4a). Compared to the more symmetric environment of 10 Se atoms in a bicapped distorted cube (4 at a distance of 3.642 Å, 2 at 3.637 Å, and 4 at 3.432 Å with ⟨Tl–Se⟩ = 3.557 Å, compare Table 2) the average Tl–Se distance is reduced by about 0.114 Å leading to significant stronger Tl–Se bonding interactions (⟨Tl–Se⟩ = 3.443 Å). This average Tl–Se distance is significantly lower than the sum of the ionic radii ($r(Tl^+)$ = 1.57 Å + $r(Se^2)$ = 1.98 Å = 3.55 Å (26)) indicative of covalent bonding interactions. The remaining 3 Se atoms are at 3.866 Å (2×) and 3.799 Å. The two Tl positions x 0 z are related by a center of symmetry. Therefore it is obvious that they cannot be occupied simultaneously because they are only 0.511 Å apart. Consequently it must be assumed that $TlCr_5Se_8$ has a domain structure with local symmetry *Cm*. Attempts to refine the structure in space group *Cm* leads to x and z coordinates for the Tl atom which are on the order of the estimated standard deviation. It has to be noted that the U_{ii} components of the Tl atom are still larger than the U_{ii} of the other atoms indicative of additional disorder or mobility of the Tl atoms. A reduction of the point symmetry from 2/*m* to *m* for the K atom was reported for KIn_5S_8 (27).

In this context it is of great interest that in $TlCr_5Te_8$ with a larger channel diameter the Tl atom shifted away from the central position by 0.3671 Å resulting in an asymmetric coordination of 7 Te atoms compared with the more symmetric but more distant coordination of the central position (6 at a mean distance of 3.700 Å and 4 neighbors

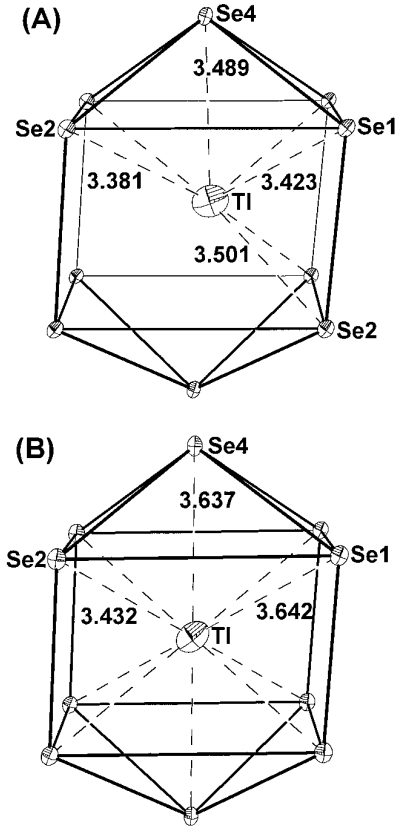

FIG. 4. Environment of the Tl atoms within the channels with Tl in x 0 z (A) and in 0 0 0 (B). Displacement ellipsoids are drawn at the 50% probability level.

TABLE 2

Selected Interatomic Distances [Å] in $Tl_xCr_5Se_8$ (x = 1, 0.78, 0.61, 0.32, and 0.077; δ = $Tl–Se_{max}–Tl–Se_{min}$; $Cr–Se_{max}–Cr–Se_{min}$)

x	1	0.78	0.61	0.32	0.077
			Tl in 0 0 0		
Tl–Se1 4×	3.642(1)	3.613(3)	3.604(1)	3.576(1)	
Tl–Se2 4×	3.432(1)	3.423(3)	3.421(1)	3.399(1)	
Tl–Se4 2×	3.637(2)	3.613(4)	3.592(2)	3.551(1)	
⟨Tl–Se⟩	3.557	3.537	3.528	3.500	3.457
δ	0.210	0.190	0.183	0.177	
			Tl in x 0 z		
Tl–Se1 2×	3.423(1)				
Tl–Se2 2×	3.381(1)				
Tl–Se2 2×	3.501(1)				
Tl–Se4	3.489(1)				
⟨Tl–Se⟩	3.443				
δ	0.120				
Cr1–Se2 2×	2.532(1)	2.527(4)	2.527(2)	2.531(1)	
Cr1–Se4 4×	2.502(1)	2.497(2)	2.498(1)	2.498(1)	
⟨Cr1–Se⟩	2.512	2.507	2.508	2.509	2.529
δ	0.030	0.030	0.029	0.033	
Cr2–Se1	2.484(1)	2.489(6)	2.475(2)	2.468(1)	
Cr2–Se4	2.551(1)	2.552(6)	2.561(2)	2.570(1)	
Cr2–Se1 2×	2.503(1)	2.495(5)	2.488(2)	2.485(1)	
Cr2–Se3 2×	2.593(1)	2.595(5)	2.592(2)	2.594(1)	
⟨Cr2–Se⟩	2.538	2.537	2.533	2.533	2.538
δ	0.109	0.106	0.117	0.126	
Cr3–Se3	2.551(2)	2.555(8)	2.551(3)	2.563(2)	
Cr3–Se4	2.513(2)	2.497(8)	2.501(3)	2.493(2)	
Cr3–Se2 2×	2.487(1)	2.484(4)	2.474(2)	2.467(1)	
Cr3–Se3 2×	2.624(1)	2.613(4)	2.619(2)	2.626(1)	
⟨Cr3–Se⟩	2.548	2.541	2.540	2.540	2.532
δ	0.137	0.129	0.145	0.159	
Cr1–Cr3	3.493(2)	3.465(5)	3.454(2)	3.427(1)	3.433(8)
Cr2–Cr3	3.058(2)	3.057(8)	3.075(2)	3.091(2)	3.166(10)
Cr2–Cr2	3.516(2)	3.501(5)	3.475(2)	3.431(2)	3.378(7)
Se1–Se1	3.532(2)	3.546(3)	3.544(2)	3.572(2)	
Se1–Se2	3.657(2)	3.619(4)	3.596(2)	3.524(2)	
Se1–Se4	3.544(2)	3.539(4)	3.536(2)	3.531(2)	
Se3–Se3	3.457(2)	3.438(4)	3.437(2)	3.429(2)	
Se2–Se4	3.517(2)	3.498(4)	3.491(2)	3.478(2)	
Se4–Se4	3.460(2)	3.468(4)	3.481(2)	3.490(2)	

Note. The data given for x = 0.077 were derived from X-ray powder Rietveld refinement.

at 3.940 Å) (14). With Tl in the central position an abnormal high B_{11} = 18.9 Å^2 was reported (14). For $TlCr_5S_8$ which has the smallest channel diameter of the three isotypic compounds we obtained a value for B_{11} of 6.8 Å^2. For this compound no reduction of the relatively high value for B_{11} was achieved by refining Tl with free varying x and z coordinates (18). These experimental results demonstrate that with increasing channel diameter the central position would lead to energetically unfavorable situations with a "rattling" Tl atom. This situation is prevented by a shift of the Tl atoms from this central position. We note that for the isotypic compounds $RbCr_5Se_8$ and $CsCr_5Se_8$ the anisotropic displacement parameters behave rather normally in agreement with the larger ionic radii of Rb^+ and Cs^+ (3).

All Tl poorer samples show high values for the U_{22} component for the Tl atoms. The U_{33} component remains unchanged and the U_{11} component decreases with decreasing Tl content. The refinement of $Tl_{0.78}Cr_5Se_8$ and $Tl_{0.61}Cr_5Se_8$ with Tl at the central position yields a high U_{22} component (B_{22} = 9.2 Å^2 for both compounds). The refinement with a freely varying y coordinate leads to a significant reduction of the U_{22} component with a large estimated standard deviation (e.s.d.) ($B_{22}(0.78)$ = 4.4(8) Å^2 and $B_{22}(0.61)$ = 3.6 (5) Å^2) and a shift of the Tl atoms from the central position by about 0.23 Å. The final R values and the U_{11} and U_{33} components are not affected. Due to the shift of the Tl atoms, a highly asymmetric environment with two short Tl–Se contacts (about 3.3 Å), 4 Se at a medium long distance (3.5–3.55 Å), and 4 Se atoms at far larger distances (3.6–3.73 Å) is observed. The average ⟨Tl–Se⟩ distances for this asymmetric coordination are only slightly larger than those obtained for Tl in the central position. Such asymmetric environments are not unusual for Tl and a displacement of Tl from y = 0 cannot be excluded. A definite decision whether the Tl atoms are mobile and/or disordered within the channels is not possible from these analyses because a high value for the U_{22} component is also expected if the crystals exhibit an inhomogeneous distribution of Tl along the channel direction, as proved for some crystals using EDAX.

For $Tl_{0.32}Cr_5Se_8$ which was obtained via a redox reaction at elevated temperatures we obtained a clearly smaller value for U_{22} (B_{22} = 4.8 Å^2). The refinement of Tl in the position 0, y, 0 leads a y coordinate with an estimated standard deviation which is 2 times larger than the value for y. Furthermore the U_{22} is not reduced but shows a high

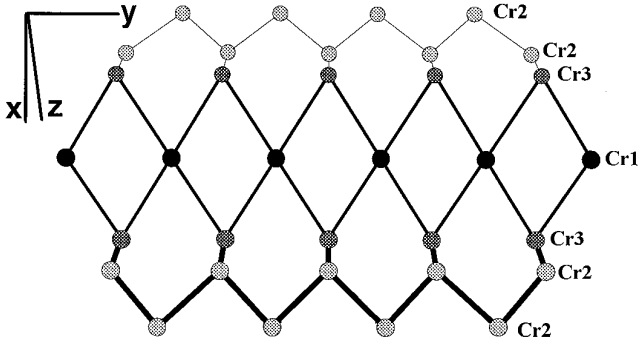

FIG. 5. The quasi-two-dimensional metal atom network in $TlCr_5Se_8$.

e.s.d. Hence in this compound Tl either oscillates about $y = 0$ and/or is statically disordered.

The detailed analysis of the anisotropic displacement components of Tl in $Tl_xCr_5Se_8$ ($0.3 \leq x \leq 0.8$) highly suggests that the unusual large values for U_{22} are the result of a superposition of disorder, mobility, and an inhomogeneous distribution of Tl atoms.

The possibility of the formation of a commensurate or incommensurate superstructure can be excluded because we observed neither additional reflections nor diffuse intensity between Bragg layers on long exposed oscillation rotation photographs about the crystallographic *b* axis ($Tl_{0.4}Cr_5Se_8$; 150 h). Such long range ordering was reported for $Tl_xV_5S_8$ (9) and $K_xV_5S_8$ (5, 28).

At this stage we want to discuss the changes of the Tl–Se interatomic distances as a function of Tl content if we assume that Tl is in the central position. The average Tl–Se distance shrinks by about 0.1 Å when *x* is reduced to 0.08 in $Tl_xCr_5Se_8$, but the individual Tl–Se bonds exhibit different alterations. In $TlCr_5Se_8$ the average Tl–Se bond length of 3.557 Å matches well with the sum of the ionic radii. For other Tl^+ containing compounds, in which Tl is in a different environment, significantly shorter Tl–Se bond lengths are reported (Tl_5Se_3 (29), Tl_4TiSe_4 (30), Tl_3PSe_4 (31), and $TlGaSe_2$ (32)).

For Tl^{3+} the ionic radius of 0.766 Å (26) is roughly one half of the radius of Tl^+. Hence, the formation of Tl^{3+} should lead to a drastic decrease of the average Tl–Se distance. For $Tl_{0.32}Cr_5Se_8$ one would expect an average Tl–Se distance of about 3.07 Å which is about 0.43 Å smaller than the value obtained during the crystal structure refinement. Typical Tl–Se bond lengths for Tl^{3+} are 2.68 Å (TlSe (33)), 2.60 Å ($TlInSe_2$ (34)) or 2.64 Å $(Et_4N_3)_3(Tl_3Se_3(Se_4)_3)$ (35). Regardless whether the Tl occupies the central postion or not the observed Tl–Se bond distances are far too long for a Tl^{3+} ion. Hence we exclude the possibility of the formation of Tl^{3+} during the chemical redox reaction. Regarding the possible reactions paths mentioned in the Introduction the present analysis highly suggests that [a] can be left out of consideration for the present system.

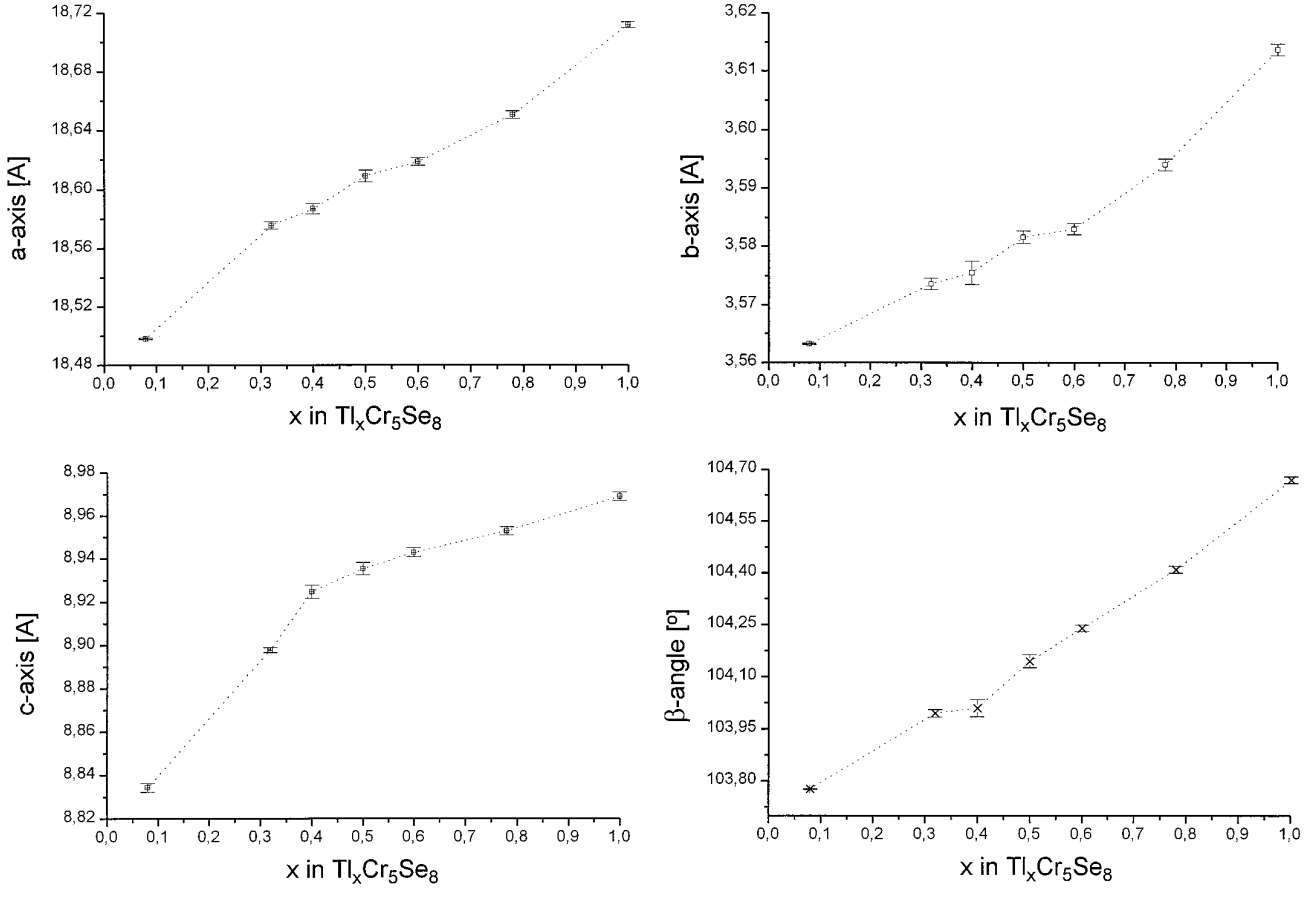

FIG. 6. Change of the lattice parameters with Tl content in $Tl_xCr_5Se_8$. Note: the data for $x \approx 0.08$ are obtained from X-ray powder Rietveld refinement.

It is also noteworthy that in the isostructural titanium and vanadium selenides the Tl atoms are in a more regular environment (1, 2). The average Tl–Se distances (coordination number 10) are 3.487 Å for $TlTi_5Se_8$ and 3.377 Å for TlV_5Se_8.

The change of the lattice parameters as a function of Tl content is displayed in Fig. 6. Within experimental accuracy, with decreasing Tl content we observe a nearly linear decrease of the *a* axis as well as of the monoclinic angle, whereas both the *b* and *c* axes change in a nonlinear fashion. The unit cell volume decreases by about 3.8% from $x = 1$ to $x = 0.08(1)$ in $Tl_xCr_5Se_8$. It is obvious from Fig. 6 that the lattice parameters contract in a very anisotropic way. The *a* axis decreases by about 0.214 Å whereas the *b* and *c* axes contract by 0.051 and 0.135 Å, respectively. Such anisotropic behavior was also found for $Tl_xV_5S_8$ (12). It is noted that our results are in conflict to the data published by Ohtani *et al.* (13). In the composition range $0.33 \leq x \leq 1$ they observed no change of the *c* axis and of the monoclinic angle β. In addition the *a* axis drops only by about 0.05 Å from 18.75 to 18.70 Å and the *b* axis shows no significant variation (13). The reasons for these contradicting results are not clear. In addition, the reported lattice parameters for Cr_5Se_8 ($a = 18.574$ Å, $b = 3.5679$ Å, $c = 8.8776$ Å, and $\beta = 104.7°$) are significantly larger than our data obtained during a full powder pattern Rietveld refinement for $Tl_{0.077(5)}Cr_5Se_8$ (compare the Experimental section and see Fig. 7). Because they assumed that the charge of the host matrix is invariable, they rejected their results. In addition they speculated that Na^+ was replaced by protons during the deintercalation reaction (13).

The anisotropic changes of the lattice parameters can be explained by an analysis of the Cr–Se and Cr–Cr interatomic distances. With decreasing Tl content the average ⟨Cr–Se⟩ distances exhibit only minute changes whereas the individual Cr–Se bonds show different alterations (see Table 2 and Fig. 8). The parameter δ defined as the difference ($Cr–Se_{max} - Cr–Se_{min}$) gives an impression for the distortion of the $CrSe_6$ octahedra. It is obvious from Table 2 that within the accuracy of the method the octahedron about Cr1 is not affected whereas the distortion of the octahedra about Cr2 and Cr3 increases with decreasing Tl content. Within a simple ionic picture the oxidation of Cr(III) to Cr(IV) should lead to a smaller average Cr^{n+} radius ($r(Cr^{3+}) = 0.615$ Å and $r(Cr^{4+}) = 0.55$ Å) (26). Assuming a constant radius for Se^{2-} the average ⟨Cr–Se⟩ bond length should be reduced by about 2.2% when *x* is lowered from 1 to about 0.3, but, as can be deduced from Table 2 and Fig. 8, the changes of the ⟨Cr–Se⟩ distances are on the order of 0.2%, much smaller than expected if Cr(III) is successively oxidized to Cr(IV).

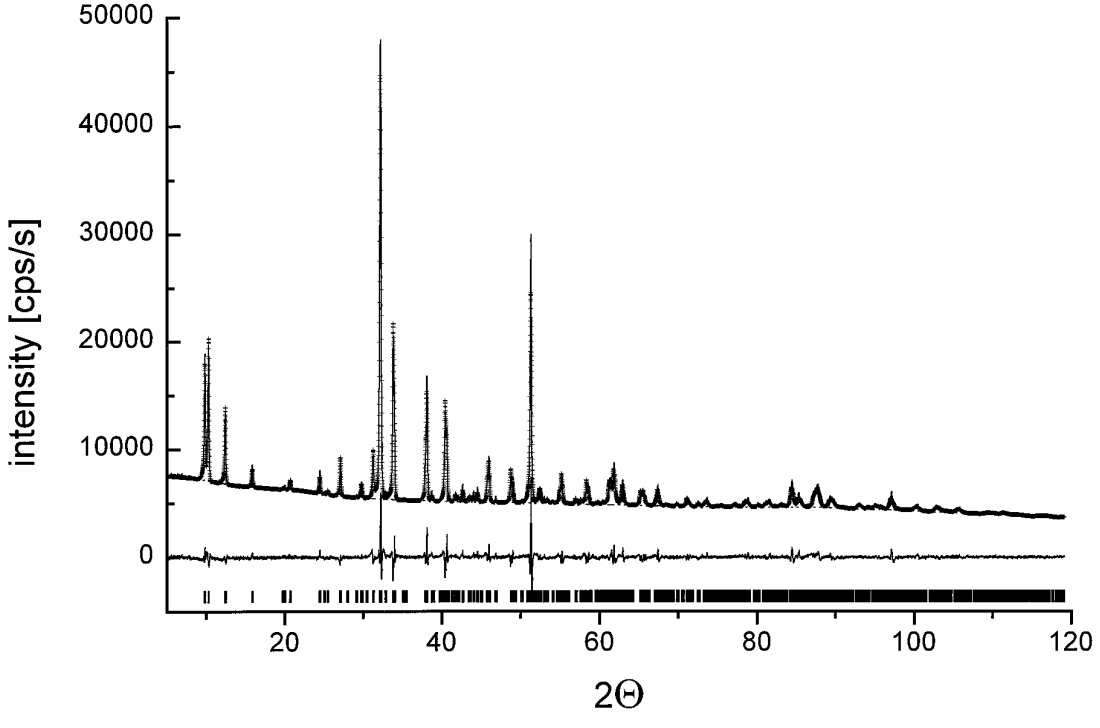

FIG. 7. Result of the Rietveld refinement performed on $Tl_{0.077}Cr_5Se_8$. The allowed reflection positions are given as horizontal bars. Measured profiles, cross; calculated profiles, line.

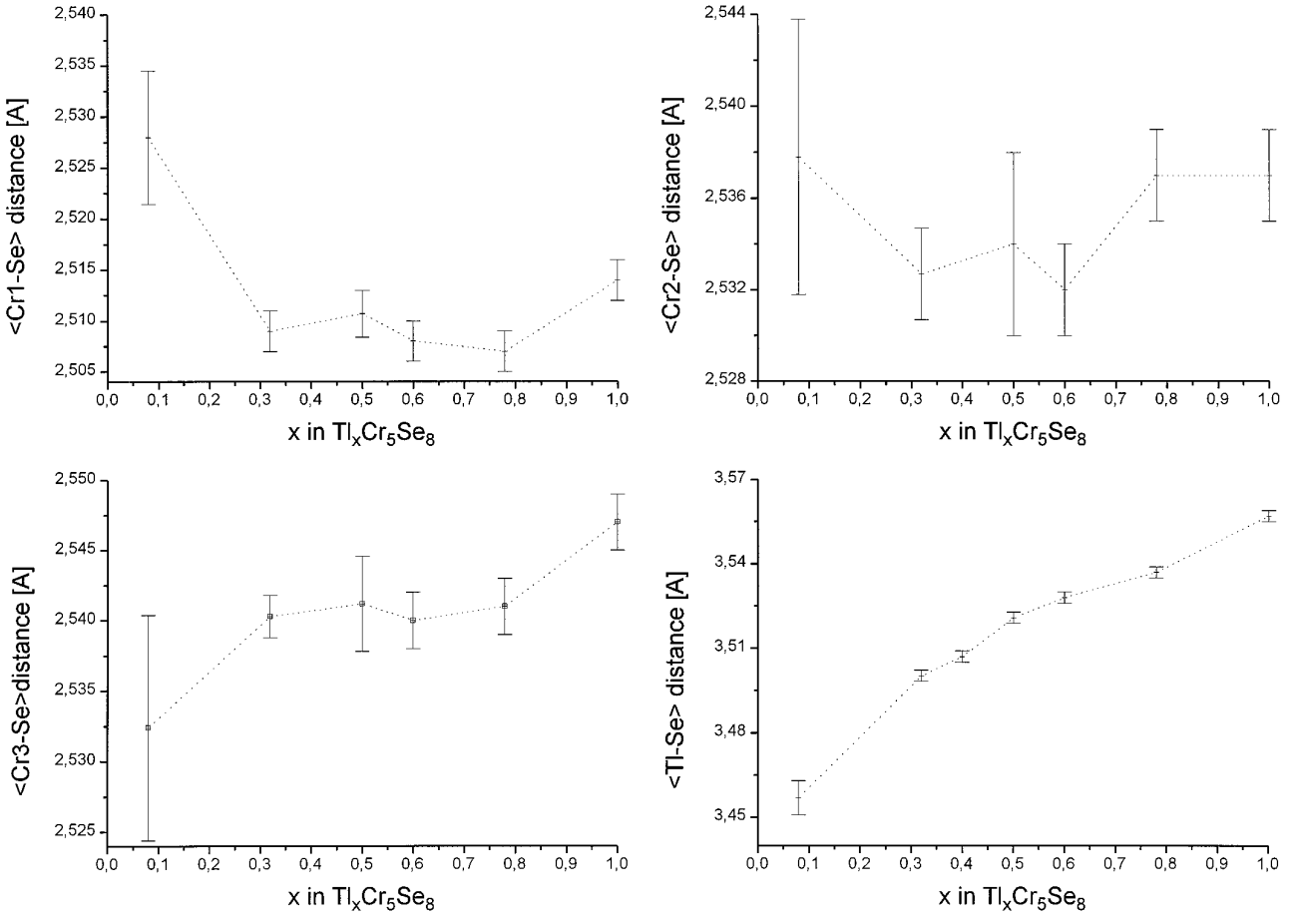

FIG. 8. Change of the average ⟨Cr–Se⟩ and ⟨Tl–Se⟩ bond distances as a function of Tl content in $Tl_xCr_5Se_8$. Note: the data for $x \approx 0.08$ are obtained from X-ray powder Rietveld refinement.

More pronounced alterations are observed for the different Cr–Cr interatomic distances. The evolution of the Cr–Cr separations as function of Tl content is shown in Fig. 9. The Crl–Cr3 and Cr2–Cr2 (common edge) separations are reduced by 0.06 and 0.138 Å, respectively. Interestingly enough the Cr2–Cr3 distance (common face) increases by 0.108 Å. These changes affect the lattice parameters in various ways. The *c* and *b* axes are influenced by the changes of the Cr2–Cr2 distance and the *c* axis is also affected by changes of the Cr2–Cr3 separation. In addition the *a* and *b* axes are sensitive to alterations of the Cr1–Cr3 interatomic distance. Because the average ⟨Cr–Se⟩ distances exhibit no significant changes as a function of Tl content (see discussion above), the anisotropic behavior of the lattice parameters are a direct consequence of the different changes of the Cr–Cr interactions.

As discussed above, the alterations of the Cr–Se bond distances gave no hints for the formation of Cr(IV). In addition, neither the Cr–Se nor the Cr–Cr interatomic distances and their changes allow a definite decision whether Cr(IV) is formed and where it would be located.

At the end of this section we discuss the change of the shortest Se–Se interatomic separations (Table 2) as function of Tl content. The shortest contacts are in the range from 3.43 to 3.657 Å, clearly longer than the distances reported for a Se–Se single bond (2.3–2.4 Å) but shorter than the sum of the ionic radii (3.90 Å). If the topotactic redox reaction proceeds after path [b2], valence band holes may be formed (36–39). In extreme cases these holes may condense leading to the formation of Se_2^{2-} pairs. But the formation of delocalized valence band holes without formation of *X–X* bonds was proposed for a number of chalcogenide spinels (36–39).

Since the alterations of the Se–Se interatomic distances are small they can be regarded as a response of the changes of the Cr–Cr interactions.

CONCLUSIONS

The topotactic redox reaction between $TlCr_5Se_8$ and bromine in acetonitrile allows the preparation of metasta-

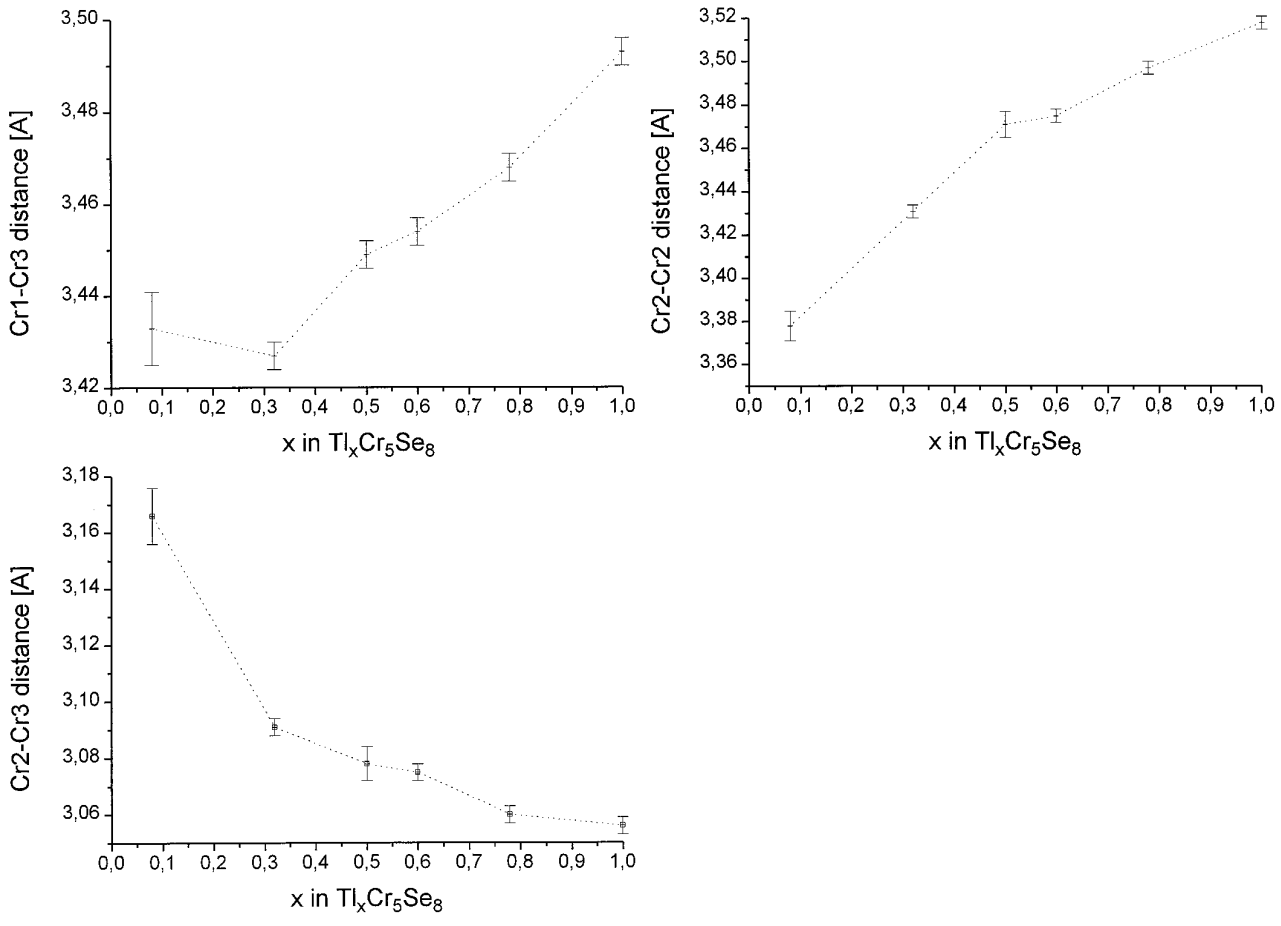

FIG. 9. Variation of the interatomic Cr–Cr bond distances in $Tl_xCr_5Se_8$ with the Tl content. Note: the data for $x \approx 0.08$ are obtained from X-ray powder Rietveld refinement.

ble compounds $Tl_xCr_5Se_8$ in the range $0 < x < 1$. The occurence of a redox reaction with electron/ion transfer can be regarded as an evidence for the electronic conductivity of the host lattice. The topotactic redox reaction is an elegant method to prepare metastable samples, which are not accessible by conventional high temperature techniques.

EDAX investigations performed on selected single crystals gave evidence for a nonuniform lateral distribution of Tl. These microinhomogeneities may also contribute to the enhanced U_{22} values, but X-ray diffraction experiments do not allow one to definitely distinguish between the different mechanisms which may be responsible for the observed changes of the magnitudes of the U_{ii} components.

The crystal structure analyses further yield some interesting and unexpected results. Especially the Cr–Cr interactions seem to play an important role for the understanding of the bonding properties in this kind of materials. The observed changes of the different Cr–Cr separations demonstrate that the removal of electrons from the host lattice mainly affect these interatomic interactions whereas the Cr–Se bonding properties are only slightly altered. This means that it is highly probable that the observed alterations of the Cr–Cr interactions in the host matrix $[Cr_5Se_8]$ are primarily correlated with the change of charge on the Cr atoms. The electronic effects dominate against geometrical alterations; i.e., changes of the ionic radii are less important for the understanding of the structural changes. The analysis of the anisotropic displacement parameters U_{ii} of Tl gives evidence for different kinds of disorder and/or mobility of the Tl atoms as a function of Tl content. In the stoichiometric compound the Tl atoms are shifted away from the central position of the channel resulting in an asymmetric environment of 7 Se atoms, but with shorter average Tl–Se distances and consequently stronger Tl–Se interactions. For the Tl poorer samples the Tl atoms are either displaced parallel to the b axis or are more mobile leading to a relatively large U_{22} component.

The results of X-ray diffraction experiments even performed on well-defined single crystals does not allow one

to definitely decide whether Cr or Se is oxidized during the redox reaction. The analysis of the Tl–Se interatomic separations only allow the exclusion of the formation of trivalent Tl. This conclusion is in accordance with the results of our photoemission experiments (40).

In two future contributions we will report the results of magnetic susceptibility measurements, low temperature X-ray single crystal structure experiments, and experimental electronic structure investigations using photoemission. All these methods clearly demonstrate that chromium is oxidized from the oxidation state Cr(III) to the unusual state Cr(IV).

ACKNOWLEDGMENTS

Financial support by the Deutsche Forschungsgemeinschaft (DFG) and by the Fonds der Chemischen Industrie (FCI) is gratefully acknowledged.

REFERENCES

1. L. Fournes, M. Vlasse, and M. Saux, *Mater. Res. Bull.* **12,** 1 (1977).
2. K. Klepp and H. Boller, *J. Solid State Chem.* **48,** 388 (1983).
3. W. Bronger, C. Herudek, J. Huster, and D. Schmitz, *Z. Anorg. Allg. Chem.* **619,** 243 (1993).
4. T. Ohtani and S. Onoue, *Mater. Res. Bull.* **21,** 69 (1986).
5. K. D. Bronsema, R. Jansen, and G. A. Wiegers, *Mater. Res. Bull.* **19,** 555 (1984).
6. W. Schramm, R. Schöllhorn, H. Eckert, and W. Müller-Warmuth, *Mater. Res. Bull.* **18,** 1283 (1983).
7. T. Ohtani and S. Onoue, *J. Solid State Chem.* **59,** 324 (1985).
8. J. Huster, *Z. Anorg. Allg. Chem.* **447,** 89 (1978).
9. H. Boller and R. Quint, *Solid State Ionics* **28–30,** 254 (1988).
10. R. Quint and H. Boller, *Mater. Res. Bull.* **22,** 1499 (1987).
11. W. Bensch and E. Wörner, *Mater. Res. Bull.* **28,** 1005 (1993).
12. W. Bensch and E. Wörner, *Solid State Ionics* **58,** 275 (1992).
13. T. Ohtani, Y. Sano, K. Kodoma, S. Onoue, and H. Nishihara, *Mater. Res. Bull.* **28,** 501 (1993).
14. H. Boller, K. O. Klepp, and K. Kirchmayr, *Mater. Res. Bull.* **30,** 365 (1995).
15. T. Novet, M. Wagner, M. Jiang, and D. C. Johnson, *Mater. Res. Bull.* **30,** 65 (1995).
16. W. Bensch, E. Wörner, M. Muhler, and U. Ruschewitz, *Eur. J. Solid State Inorg. Chem.* **30,** 645 (1993).
17. W. Bensch, E. Wörner, and P. Hug, *Solid State Commun.* **86,** 165 (1993).
18. W. Bensch, E. Wörner, and U. Ruschewitz, *J. Solid State Chem.* **110,** 234 (1994).
19. W. Bensch, E. Wörner, and M. Muhler, *Mater. Res. Bull.* **29,** 155 (1993).
20. W. Bensch, E. Wörner, and F. Tuczek, *Mater. Res. Bull.* **30,** 1065 (1995).
21. R. Schöllhorn, *in* "Proc. Int. Conf., Triest," (L. Pietronero and E. Tosatti, Eds.), p. 33. Springer-Verlag, Berlin, 1981.
22. H. Nishihara, T. Ohtani, and S. Onoue, *Europhys. Lett.* **8,** 189 (1989).
23. H. Nishihara, S. Onoue, T. Ohtani, and H. Yasuoka, *J. Magn. Magn. Mater.* **70,** 225 (1987).
24. J. Koy and W. Bensch, in preparation.
25. R. Schöllhorn, *Pure Appl. Chem.* **56,** 1739 (1984).
26. R. D. Shannon, *Acta Crystallogr. A* **32,** 751 (1976).
27. H. J. Deiseroth, *Z. Kristallogr.* **177,** 307 (1986).
28. K. D. Bronsema and J. Mahy, *Phys. Stat. Sol. A* **104,** 603 (1987).
29. L. I. Man, V. S. Parmon, R. M. Imamov, and A. S. Avilov, *Sov. Phys. Crystallogr.* **25,** 614 (1980).
30. K. O. Klepp and G. Eulenberger, *Z. Naturforsch. B* **39,** 705 (1984).
31. R. W. Alkire, P. J. Vergamini, A. C. Larson, and B. Morosin, *Acta Crystallogr. C* **40,** 1502 (1984).
32. D. Müller and H. Hahn, *Z. Anorg. Allg. Chem.* **438,** 258 (1978).
33. L. I. Man, R. M. Imanov, and S. A. Semiletov, *Sov. Phys. Crystallogr.* **21,** 355 (1976).
34. D. Müller, G. Eulenberger, and H. Hahn, *Z. Anorg. Allg. Chem.* **398,** 207 (1973).
35. S. S. Dhingra and M. G. Kanatzidis, *Inorg. Chem.* **32,** 1350 (1993).
36. A. Payer, M. Schmalz, W. Paulus, R. Schöllhorn, R. Schögl, and C. Ritter, *J. Solid State Chem.* **98,** 71 (1992).
37. A. Payer, M. Schöllhorn, R. Schlögl, and C. Ritter, *Mater. Res. Bull.* **25,** 515 (1990).
38. A. Payer, R. Schöllhorn, C. Ritter, and W. Paulus, *J. Alloys Comp.* **191,** 37 (1993).
39. A. Payer, A. Kamlowski, and R. Schöllhorn, *J. Alloys Comp.* **185,** 89 (1992).
40. W. Bensch, O. Helmer, and M. Muhler, in preparation.